49th AIAA/ASME/ASCE/AHS/ASC Structures, Structural Dynamics, and Materials Conference
 16t
7 - 10 April 2008, Schaumburg, IL

AIAA 2008-1723

A Hybrid Uncertainty Propagation Scheme for Convective Heat Transfer Problems

Paul Constantine* and Alireza Doostan †
and Gianluca Iaccarino ‡
Stanford University, Stanford CA, 94305

A computational analysis of convective heat flux around an array of cylinders in a high Reynolds number flow is presented; we assume that both the inflow and the wall heat flux conditions are specified with a margin of uncertainty and our objective is to quantify the resulting effect on some functional of interest, mainly the cylinder wall temperature. We introduce a hybrid uncertainty propagation technique that combines the accuracy and convergence properties of intrusive stochastic Galerkin with the non-intrusive nature of stochastic collocation. Additionally, it dramatically reduces the overall cost of computing the statistics of the stochastic output quantities. The success of the hybrid technique suggests future directions in loosely coupled multi-physics applications.

I. Introduction

Recent developments in numerical techniques for problems with stochastic inputs have spurred interest in several areas, including uncertainty quantification. These techniques assume that uncertain quantities in engineering models – particularly partial differential equation models – can be formulated in probabilistic terms. The uncertain quantities are then propagated through the physical domain, and their effects on the outputs are "quantified". Using classical respresentations such as Wiener-Hermite expansions for the probabilistic quantities, one may readily compute statistics – expectation, variance, probability density functions – of output quantities of interest.

Non-intrusive techniques – such as Monte Carlo and stochastic collocation[8] – are particularly appealing as a method of computation since, by definition, they do not require any alterations to *trusted* deterministic solvers. However, these methods can suffer from poor convergence behavior and/or an exponential increase in computational cost as the number of input parameters increases. Some variants have even been shown to produce inadmissible results such as negative values for variance.[2] In contrast, the intrusive techniques – such as intrusive stochastic Galerkin schemes – require modifications to existing solvers but promise highly accurate, rapidly converging statistics.

In this paper, we pursue a hybrid technique that achieves the accuracy of intrusive stochastic Galerkin while retaining a *largely* non-intrusive implementation. The technique we present is derived for a high Reynolds number model of turbulent flow and heat transfer around cylinders; it is based on the Reynolds-Averaged Navier Stokes (RANS) equations in the limit of incompressible flow. The decoupling of the momentum from the energy transport is exploited by using different techniques to propagate the uncertainty in each of the physical components; this leads to large savings in computational cost compared to *conventional* propagation techniques. We anticipate that similar hybrid techniques can be derived for other loosely coupled multi-physics problems.

II. Problem Description

In previous work,[2] we describe the present problem of turbulent flow and heat transfer past an array of cylinders. The motivation comes from the design of cooling systems in turbine blades of modern jet engines.

*Ph.D. Candidate, Institute for Computational and Mathematical Engineering
†Research Associate, Center for Turbulence Research
‡Associate Professor, Mechanical Engineering

These cooling systems consist of very intricate secondary flow passages; current designs include an array of cylindrical pins that assist in cooling the trailing edge region of the blade. The configuration analyzed here includes a periodic array of pins separated by a distance $L/D = 1$ (where D is the cylinder diameter). The flow conditions are assumed to be fully turbulent with a Reynolds number based on the incoming fluid stream (and D) of $Re_D = 1,000,000$. In this regime, direct simulations of the length and time scales of the flow are impractical due to the extremely large computational cost and we resort to Reynolds-Averaged modeling.

The focus of the present investigation is to study the effect of *uncertainty* in the problem definition of the heat flux on the cylinder wall. We do not comment on the overall accuracy of the heat flux predictions as they might be affected by the RANS modeling closure.

Typically, the presence of intricate secondary flow passages and structure/fluid interactions upstream of the pin array create complex inflow conditions. Rather than attempting to describe such complexities, we model the inflow velocity as an *uncertain*, spatially varying function parameterized by two uniform random variables (see equation (4)). An additional source of uncertainty for this problem occurs in the specification of the heat flux boundary condition on the cylinder wall. It is possible, in principle, to simulate the conjugate (solid and fluid) heat transfer problem, but this would require physical coupling between the pins and surrounding components to correctly identify the heat *flow*. It is common practice to perform simulations by assuming a constant heat flux condition on the cylinder wall so that the problem remains simple and confined. In an attempt to identify the possible limitations of the above assumption, we model the heat flux boundary as an *uncertain*, spatially varying function parameterized by one uniform random variable (see equation (5)).

Mathematically, the problem can be described as follows. The computational domain is shown in figure 1. The equations describing the Reynolds averaged temperature (T) and velocity (U_i) are the two-dimensional

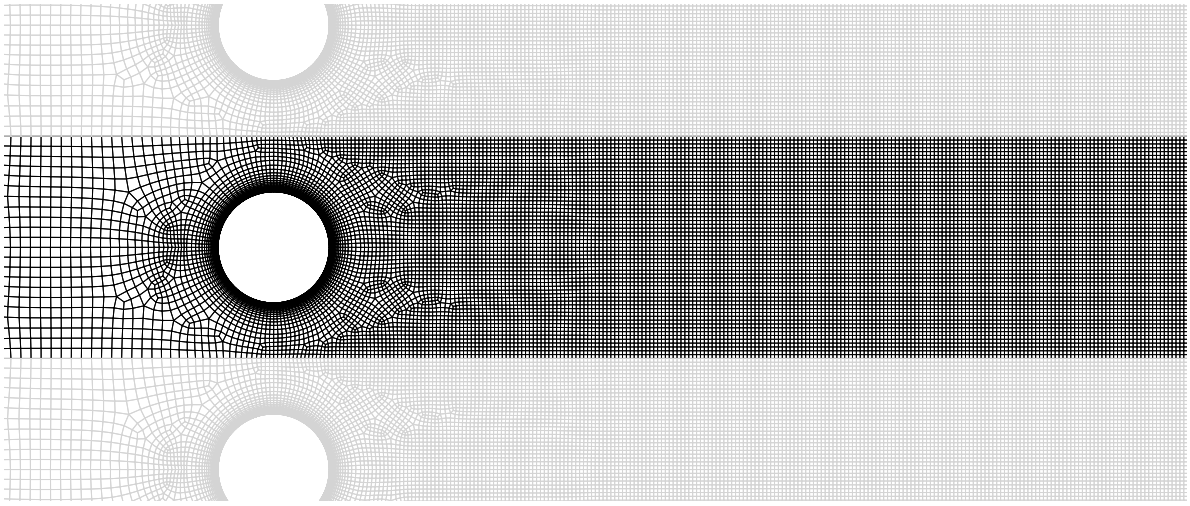

Figure 1. Unstructured grid used in the present computations showing the strong clustering at the cylinder surface to capture the boundary layer. The dark region is the actual computational domain: periodic conditions are used on the upper and lower boundary.

RANS equations written in the assumption of incompressible fluid (constant density) and steady flow.

$$\frac{\partial U_i}{\partial x_i} = 0 \tag{1}$$

$$U_j \frac{\partial U_i}{\partial x_j} = \frac{\partial}{\partial x_j}\left[(\nu + \nu_t)\frac{\partial U_i}{\partial x_j}\right] - \frac{1}{\rho}\frac{\partial P}{\partial x_i} \tag{2}$$

$$U_j \frac{\partial T}{\partial x_j} = \frac{\partial}{\partial x_j}\left[\left(\kappa + \frac{\nu_t}{Pr_t}\right)\frac{\partial T}{\partial x_j}\right] \tag{3}$$

where the density (ρ), the molecular viscosity (ν) and the thermal conductivity (κ) are *constant* and given properties of the fluid. The eddy viscosity (ν_t) is computed using the k-ω turbulence model,[4] and the

turbulent Prandtl number (Pr_t) is assumed to be a constant. The energy equation is decoupled from the momentum equation and can be solved after the velocity field is computed.

The uncertain boundary conditions are parameterized by a total of three independent uniform random variables, Y_1, Y_2, and Y_3, with support $[-1, 1]$. One can think of each of these random variables as an additional coordinate dimension that influences the quantities of interest.

The inlet velocity profile is constructed as a linear combination of two cosine functions of $x_2 \in [-2, 2]$, i.e.

$$U_{inlet}(x_2, Y_1, Y_2) = 1 + \sigma_1(Y_1 \cos(2\pi x_2) + Y_2 \cos(10\pi x_2)). \tag{4}$$

where σ_1 controls the inflow velocity fluctuations. For numerical experiments, we set $\sigma_1 = 0.25$, which ensures that the amplitude of the random fluctuations does not cause the inlet velocity to become negative. This model allows moderate random fluctuations about a mean value, $\mathbf{E}[U_{inlet}] = 1$, where $\mathbf{E}[\cdot]$ is the mathematical expectation operator. The wave numbers 2 and 10 in (4) were chosen to introduce low and high frequency fluctuations, respectively, while maintaining symmetry in the problem about $x_2 = 0$.

The heat flux on the cylinder wall is specified as an exponential function of Y_3 over the domain $x_1 \in [-0.5, 0.5]$ for each value of Y_3, namely

$$\left.\frac{\partial T}{\partial n}\right|_{cylinder} (x_1, Y_3) = e^{-(0.1+\sigma_2 Y_3)(x_1 - 0.5)} \tag{5}$$

where n is the normal to the cylinder and σ_2 controls the influence of Y_3. For the numerical experiments, we chose $\sigma_2 = 0.05$. The heat flux is greater at the left side of the cylinder where flow strikes it; the value of Y_3 determines precisely how much greater.

The randomness in the boundary conditions induces randomness in the output velocity field $U(\mathbf{x}, Y_1, Y_2, Y_3)$ and temperature $T(\mathbf{x}, Y_1, Y_2, Y_3)$. The goal of our computations is then to compute statistics – specifically expectation and variance – of the random output quantities in order to *quantify the uncertainty* in the system. Note that the decoupling of the momentum from the energy transport implies $T(\mathbf{x}, Y_1, Y_2, Y_3) = T(\mathbf{x}, U(Y_1, Y_2), Y_3)$, which is crucial to the formulation of our hybrid stochastic collocation/intrusive stochastic Galerkin scheme propagation technique. To compute statistics, we implement the hybrid technique and compare its properties to a stochastic collocation scheme.

III. Uncertainty propagation techniques

In this section we briefly describe the techniques of stochastic collocation and stochastic Galerkin for computing statistics of differential equation models with random inputs. Many excellent papers are currently available that describe and analyze these techniques in detail; we include this description for completeness. For notational consistency, we introduce an abstract problem to describe these methods in a general setting. Assume the randomness in the model can be characterized by a set of $d < \infty$ independent random variables denoted $Y = \{Y_1, \ldots, Y_d\}$ defined on some appropriate probability space, and let $D \subset \mathbb{R}^N$ be a bounded domain with boundary ∂D. We seek a stochastic solution $u(x, Y)$ that satisfies

$$\mathcal{L}(x, Y; u) = f(x, Y) \qquad x \in D, \tag{6}$$

subject to the boundary conditions

$$\mathcal{B}(x, Y; u) = g(x, Y) \qquad x \in \partial D. \tag{7}$$

Here $\mathcal{L}$ is a differential operator and $\mathcal{B}$ is a boundary operator; we assume that this problem is well-posed.

III.A. Stochastic Collocation

Integration and interpolation are the fundamental concepts behind the class of uncertainty quantification techniques known as stochastic collocation schemes,[8] which were originally developed in the context of partial differential equation models with stochastic inputs. Much of the work in this context has focused on the problem of high-dimensional parameter spaces[6] where multi-dimensional interpolation and integration can have a computational cost that increases exponentially with the dimension of the parameter space; the so-called curse of dimensionality.

As in classical numerical integration and interpolation, one can approximate the desired statistics by evaluating the unknown function (i.e. solving the differential equations) at a finite set of parameter values. This reduces the full stochastic problem to a set of uncoupled deterministic problems: For $k = 1, \ldots, K$ choose $Y^{(k)}$ from the range of Y according to a multi-dimensional interpolation or integration formula. Then solve K deterministic problems of the form

$$\mathcal{L}(x, Y^{(k)}; u^{(k)}) = f(x, Y^{(k)}) \qquad x \in D, \tag{8}$$

with boundary conditions

$$\mathcal{B}(x, Y^{(k)}; u^{(k)}) = g(x, Y^{(k)}) \qquad x \in \partial D. \tag{9}$$

The computed solutions $\{u^{(k)}\}$ corresponding to $Y^{(k)}$ are used to compute statistics of the stochastic solution $u(x, Y)$ with the interpolation and integration formulas. This technique is therefore called *non-intrusive*, since the practitioner may use existing, optimized deterministic solvers. Note that the integration and interpolation occur along the coordinates induced by the components of Y, where the number of components d in Y gives the number of dimensions of the interpolation and integration.

III.A.1. Interpolation and Integration

For a one dimensional function $f(y)$ defined on $[-1, 1]$, we define an interpolation operator $\mathcal{U}^i$ as

$$\mathcal{U}^i(f)(y) = \sum_{j=1}^{m_i} f(y_j^i) l_j(y),$$

where $l_j(y) = \prod_{k=1,\, k\neq j}^{m_i} \frac{y - y_k^i}{y_j^i - y_k^i}$ is the Lagrange polynomial of degree $m_i - 1$. The interpolant $\mathcal{U}^i(f)$ is unique and equals $f(y)$ at each point in the abscissa $\{y_1^i, \ldots, y_{m_i}^i\}$.

The natural extension of interpolation to multiple dimensions is a tensor product of one-dimensional interpolants. Let $F(y_1, \ldots, y_d)$ be defined on the hypercube $\Gamma = [-1, 1]^d$. Following standard notation, we introduce a multi-index $\mathbf{i} = (i_1, \ldots, i_d)$. The set of points for the multi-dimensional interpolant is the tensor product of the abscissas for the one-dimensional interpolants:

$$\{y_1^{i_1}, \ldots, y_{m_{i_1}}^{i_1}\} \times \cdots \times \{y_1^{i_d}, \ldots, y_{m_{i_d}}^{i_d}\}$$

Note that the number of points in the abscissa is $m_{i_1} m_{i_2} \cdots m_{i_d}$, which increases exponentially as d increases. We construct the full tensor product interpolant as

$$\mathcal{I}_{\mathbf{i}} = (\mathcal{U}^{i_1} \otimes \cdots \otimes \mathcal{U}^{i_d})(F) = \sum_{j_1=1}^{m_{i_1}} \cdots \sum_{j_d=1}^{m_{i_d}} F(y_{j_1}^{i_1}, \ldots, y_{j_d}^{i_d})(l_{j_1}^{i_1} \otimes \cdots \otimes l_{j_d}^{i_d}). \tag{10}$$

To approximate integrals of $F(y_1, \ldots, y_d)$, one needs only to integrate the interpolating basis polynomials; this yields the so-called interpolatory quadrature rules. In the classical literature on numerical integration, it is well-known that the Gauss points maximize the degree of polynomial that the integration rule can integrate exactly. Specifically, an n-point Gaussian quadrature rule can exactly integrate a polynomial of degree $2n - 1$. This *degree of exactness* extends to the tensor product case in a natural way.

Remark: The clear downfall of the tensor construction is the exponential increase in the number of points as the dimension increases. To combat this, some have proposed using a sparse grid construction in multiple dimensions based on one dimensional Clenshaw-Curtis integration formulas.[5,6,8] However, we have argued that for our particular problem, the statistics computed on the tensor grid are much more accurate than those computed on a sparse grid at a comparable computational cost.[2] For some quantities, the sparse grid statistics return inadmissible values, such as negative values for variance. Therefore we do not pursue the sparse grid approaches further in this paper.

III.B. Stochastic Galerkin

Another technique to compute statistics of the stochastic solution $u(x, Y)$ is the stochastic Galerkin method. This technique utilizes a specific representation of the random quantities called the polynomial chaos expansion (PCE). The PCE expresses a random quantity as an infinite series of orthogonal polynomials that take

a vector of random variables as arguments. This representation has its roots in the work of Wiener[10] who expressed a Gaussian process as an infinite series of Hermite polynomials. In the early 1990s, Ghanem and Spanos[7] truncated Wiener's representation to finitely many terms and used the resulting truncated PCE as a primary component of their stochastic finite element method; this truncation made computations possible. In 2002, Xiu and Karniadakis[9] expanded this method to chaos representations with bases that are orthogonal with respect to non-Gaussian probability measures.

To introduce the method, consider the space $\hat{\Pi}_k$ of polynomials in Y of univariate monomial degree not exceeding k. Let Π_k represent the set of all polynomials in $\hat{\Pi}_k$ that are orthogonal to $\hat{\Pi}_{k-1}$, and let $\Psi_k(Y) \in \Pi_k$. The orthogonality of the spaces Π_k implies

$$\mathbf{E}[\Psi_j(Y), \Psi_k(Y)] \equiv \int_\Gamma \Psi_j(y)\Psi_k(y)W(y)\,dy = h_k\delta_{jk} \text{ for } j,k \geq 0.$$

where $W(y)$ is the joint probability density function of Y, h_k is a constant, and δ_{jk} is the Kronecker delta. It can be shown[7] that any $u(x,Y) \in L_2(Y)$ admits the following representation:

$$u(x,Y) = \sum_{j=0}^{\infty} u_j(x)\Psi_j(Y). \tag{11}$$

Equation (11) is called the polynomial chaos expansion (PCE), and $\{u_j\}$ are the PCE coefficients. By the Cameron-Martin theorem,[1] this series converges in an $L_2(Y)$ sense, i.e.

$$\mathbf{E}\left[\left(u - \sum_{j=0}^{M} u_j\Psi_j\right)^2\right] \to 0$$

as $M \to \infty$. The L_2 convergence of this expansion motivates an approximate representation of $u(x,Y)$ by truncating the series (11) after $M < \infty$ terms. In other words, we can approximate u with the finite series

$$u(x,Y) \approx \sum_{j=0}^{M} u_j(x)\Psi_j(Y). \tag{12}$$

The value of M is determined by the number d of components in Y and the highest order p of polynomial in $\{\Psi_j\}$ with the formula

$$M = (d+p)!/(d!p!). \tag{13}$$

In practice, d is a modeling choice (or requirement) and p is chosen according to a variety of factors including desired accuracy of statistics and available computational resources. With the truncated PCE, the problem of solving for $u(x,Y)$ transforms into the problem of computing its coefficients $\{u_j(x)\}$.

The orthogonal basis polynomials $\{\Psi_j(Y)\}$ are chosen according to the joint probability density function of Y.[9] For example, in the case where Y is a vector of independent uniform random variables, the $\{\Psi_j(Y)\}$ are the multi-dimensional Legendre polynomials. The proper choice of basis can greatly enhance the convergence properties of the statistics.

To compute the coefficients $\{u_j(x)\}$, one can substitute the expansion (12) into (6)-(7) and project the resulting equation onto each basis polynomial $\Psi_k(Y)$.

$$\mathbf{E}\left[\mathcal{L}\left(x, Y; \sum_{j=0}^{M} u_j\Psi_j\right), \Psi_k\right] = \mathbf{E}[f(x,Y), \Psi_k] \tag{14}$$

$$\mathbf{E}\left[\mathcal{B}\left(x, Y; \sum_{j=0}^{M} u_j\Psi_j\right), \Psi_k\right] = \mathbf{E}[g(x,Y), \Psi_k] \tag{15}$$

The orthogonality of $\{\Psi_j\}$ leaves a set of $M+1$ coupled equations for $\{u_j\}$. Once solved, statistics of the stochastic solution $u(x,Y)$ can be approximated by simple formulas of $\{u_j\}$. While the stochastic Galerkin technique has been shown to produce highly accurate statistics, it often requires that existing solvers be modified to solve for the coefficients of the expansion.

IV. A hybrid propagation technique

We now depart from the general differential equation given by (6)-(7) and return to the problem of interest given by equations (1)-(3) to describe the hybrid technique. Before delving into details, we mention our deterministic solver; an important part of any implementation of a non-intrusive propagation technique is the deterministic solver. For a particular realization of (Y_1, Y_2, Y_3), we employ the commercial software package Fluent[3] to solve for the temperature and velocity fields in the Reynolds-averaged Navier Stokes equations. Fluent uses a finite volume second-order discretization on unstructured grids. The mesh has been generated to achieve high resolution of the boundary layer on the cylinder surface with $y^+ \approx 1$. We performed preliminary simulations to assess the resolution requirements for the present problem. Each deterministic solve is converged to steady state by ensuring that the residuals of all the equations are reduced by four orders of magnitude.

One motivation for pursuing a hybrid technique came from the observation[2] that the quantity with the highest variability was the temperature at the the front of the cylinder, i.e. the stagnation point of the flow. Some non-intrusive stochastic collocation variants have difficulty accurately capturing this high variability, so we investigated an accurate stochastic Galerkin representation for the temperature while retaining the stochastic collocation representation of the velocity with its non-intrusive implementation. This is facilitated problem by the decoupling of the velocity from the temperature in equations (1)-(3), which implies that the uncertainty introduced in the thermal boundary condition does not influence the velocity distribution. Since the thermal boundary condition is a function of Y_3, the velocity is therefore a function of only Y_1 and Y_2, i.e. $U = U(\mathbf{x}, Y_1, Y_2)$. This means we can treat equation (2) using a stochastic collocation scheme in only *two* dimensions.

To handle the energy equation (3), we use a truncated polynomial chaos expansion of temperature in *only* the component Y_3.

$$T(\mathbf{x}, Y_1, Y_2, Y_3) \approx \sum_{k=0}^{M} T_k(\mathbf{x}, Y_1, Y_2)\Psi_k(Y_3), \tag{16}$$

where the uniform distribution of Y_3 implies that the $\{\Psi_k\}$ are the one-dimensional Legendre polynomials with support $[-1, 1]$ and weight function $W = 1/2$. Substituting this representation into (3) and performing the Galerkin projection along the component Y_3 yields $M + 1$ distinct equations for the coefficients T_k.

$$U_j \frac{\partial T_k}{\partial x_j} = \frac{\partial}{\partial x_j}\left[\left(\kappa + \frac{\nu_t}{Pr_t}\right)\frac{\partial T_k}{\partial x_j}\right], \quad k = 0, \ldots, M \tag{17}$$

The flux boundary conditions for these equations follow from the Galerkin projection applied to the boundary condition (5).

$$\left.\frac{\partial T_k}{\partial n}\right|_{cylinder} = \frac{\mathbf{E}[e^{-(0.1+\sigma Y_3)(x_2-0.5)}\Psi_k]}{\mathbf{E}[\Psi_k^2]} \tag{18}$$

Since (3) is linear and the dependence on Y_3 occurs only at the boundary condition, the equations for T_k naturally decouple. Thus the problem reduces to the continuity and momentum equations – dependent on the random variables Y_1 and Y_2 – and a set of uncoupled scalar transport equations for the coefficients T_k – also dependent on Y_1 and Y_2. We can solve these equations non-intrusively as before using a stochastic collocation scheme with Fluent as the deterministic solver.

To approximate the expectation and variance of the original temperature and velocity fields, we compute

$$\mathbf{E}[U_j](\mathbf{x}) \approx \frac{1}{4}\sum_{l=0}^{m} U_j(\mathbf{x}, Y_1^{(l)}, Y_2^{(l)})w_l \tag{19}$$

$$\equiv \mu_{U_j}(\mathbf{x}) \tag{20}$$

$$\mathbf{E}[T](\mathbf{x}) \approx \frac{1}{4}\sum_{l=0}^{m} T_0(\mathbf{x}, Y_1^{(l)}, Y_2^{(l)})w_l \tag{21}$$

$$\equiv \mu_T(\mathbf{x}) \tag{22}$$

$$\mathbf{Var}[U_j](\mathbf{x}) \approx \frac{1}{4}\sum_{l=0}^{m} U_j(\mathbf{x}, Y_1^{(l)}, Y_2^{(l)})^2 w_l - \mu_{U_j}(\mathbf{x})^2 \tag{23}$$

$$\mathbf{Var}[T](\mathbf{x}) \approx \frac{1}{4}\sum_{l=0}^{m} \left(\sum_{k=0}^{M} T_k(\mathbf{x}, Y_1^{(l)}, Y_2^{(l)})^2 \mathbf{E}[\Psi_k^2]\right) w_l - \mu_T(\mathbf{x})^2 \tag{24}$$

where the $(Y_1^{(l)}, Y_2^{(l)}, w_l)$ come from the m-point tensor-product quadrature rule.

The choice of the problem results in physical decoupling of the $\{T_k\}$ as a consequence of the loose coupling between temperature and velocity. For the fully coupled model where the momentum equation includes the temperature in the forcing term, the equations for $\{T_k\}$ are coupled, and we cannot simply use Fluent to solve a set of transport equations with each deterministic solve. However, we expect the present approach to be useful in different situations where the physical models are either naturally decoupled or only loosely coupled to the main flow transport such as, for example pollutant dispersion problems.

From a practical perspective, we have replaced a dimension in the probability space by a set of uncoupled equations in physical space, and this has greatly reduced the total cost of the computation. This was an unexpected benefit, since we were primarily aiming for greater accuracy instead of reduced cost. But it suggests that there may be other similar hybrid approaches that improve the computational cost at a mild expense in accuracy.

V. Results

In this section, we present numerical results that compare the hybrid method against a converged Monte Carlo method and a high order stochastic collocation scheme. The Monte Carlo results use 10,000 samples. We consider this number of deterministic solves unrealistic for complex flow problems of interest, but the efficiency of the Fluent solves allowed us to use this technique to verify the stochastic collocation and hybrid techniques.

To motivate the numerical experiments, we first compute the conditional variance of the temperature given $Y_1 = Y_2 = 0$, and compare it to the Monte Carlo results. This conditional variance can be computed from a single deterministic solve that includes the transport equations for T_k, i.e.

$$\mathbf{Var}[T(\mathbf{x}, Y_1, Y_2, Y_3) \mid Y_1 = Y_2 = 0] = \sum_{k=1}^{M} T_k(\mathbf{x}, 0, 0)^2 \mathbf{E}[\Psi_k^2] \tag{25}$$

In figure 2 we plot the conditional variance against the Monte Carlo variance on the wall of the cylinder (2(b)) and along the centerline of the domain immediately before the stagnation point of the flow (2(a)). We note that the conditional variance is much smaller than the Monte Carlo variance, which suggests that the total variance in temperature has *significant* contributions from the variability in Y_1 and Y_2. Thus we are justified in pursuing the full hybrid computation. In both the hybrid and the stochastic collocation, we build the multi-dimensional quadrature formulas from 9-point Gaussian quadrature along each component. The number of deterministic solves for the stochastic collocation with three random parameters is 729, and the number of deterministic solves in the hybrid approach (where each solve includes the transport equations for $\{T_k\}$) with two random parameters is 81. We use a fourth order expansion ($M = 4$) of T along the component Y_3. One deterministic solve including the extra scalar transport equations is approximately 60% more expensive to complete than a solve with no extra scalars.

In addition to a large temperature variance at the stagnation point, fig. (2(b)) illustrates that the uncertainty is considerably higher in the boundary layer upstream of the separation ($x_1 \approx .1$) than in the downstream area. This is expected since the variability in the upstream conditions does not *penetrate* the separated shear layer (the location of the flow separation is only a function of the Reynolds number, which is not considerably altered by the varying inflow conditions) and the wall heat flux is mostly uncertain at the stagnation point (Eq. 5).

In figure 3 we plot the expectation and variance of the x_1-velocity along the centerline of the domain. The recirculation region of the flow in the wake of the cylinder is clearly visible in the expectation, and the variance plot shows that the variability in the x_1-velocity decreases dramatically after the cylinder. All methods agree remarkably, although the agreement between the hybrid and the full stochastic collocation is expected by construction; the velocity only depends on Y_1 and Y_2, so using stochastic collocation in all three dimensions is just extra work.

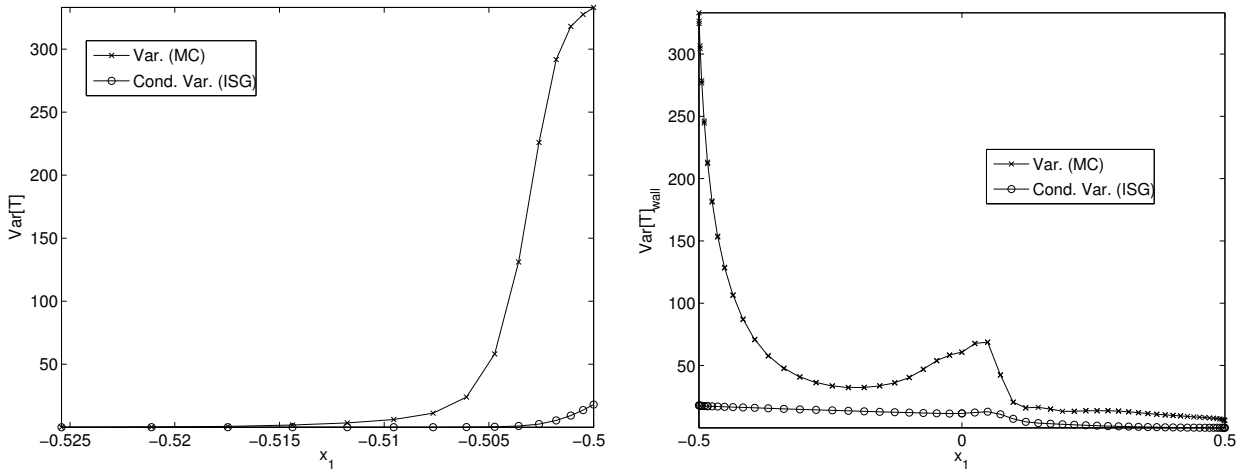

Figure 2. Conditional variance of temperature given $Y_1 = Y_2 = 0$.

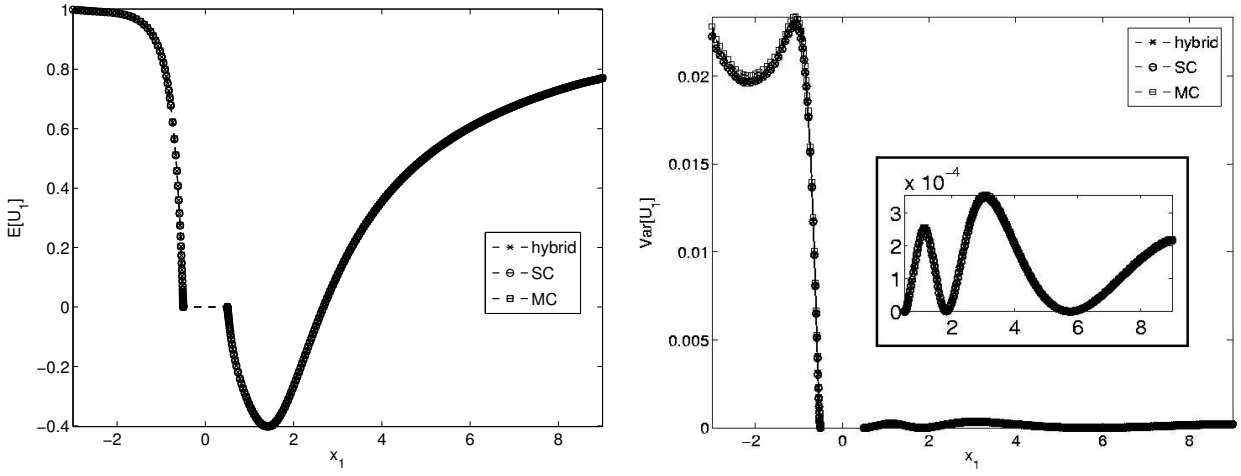

(a) Expectation

(b) Variance

Figure 3. Statistics of x_1-velocity along the domain centerline ($x_2 = 0$).

In table 1 we present the expectation and variance of the temperature at the stagnation point of the flow. Again, the results are remarkably similar considering the dramatic differences in computational cost. In figure 4 we plot the expectation and variance of the temperature on the wall of the cylinder as a function of x_1.

VI. Conclusions

We have presented a non-intrusive hybrid uncertainty propagation technique which combines stochastic collocation and stochastic Galerkin schemes to compute statistics of stochastic quantities of interest in a loosely coupled Reynolds-avereaged Navier Stokes model with uncertain boundary conditions. By expanding the temperature in a polynomial chaos expansion along one of the parameterizing random variables, we reduce the dimension of the stochastic collocation problem and introduce a set of uncoupled scalar transport equations for the coefficients of the temperature expansion. The method thus reduces the number of deterministic solves required to compute the statistics, and the results are remarkably accurate. We anticipate this method will suggest future directions for similar hybrid methods in other turbulence models. In the future, we hope to examine the rates of convergence on both the order of the polynomial chaos expansion

	hybrid	stochastic collocation	monte carlo
$\mathbf{E}[T]_{\text{stagnation}}$	150.7341	150.7623	151.0774
$\mathbf{Var}[T]_{\text{stagnation}}$	323.2077	323.0808	333.1317

Table 1. Expectation and variance of the temperature at the stagnation point of the flow at the front of the cylinder.

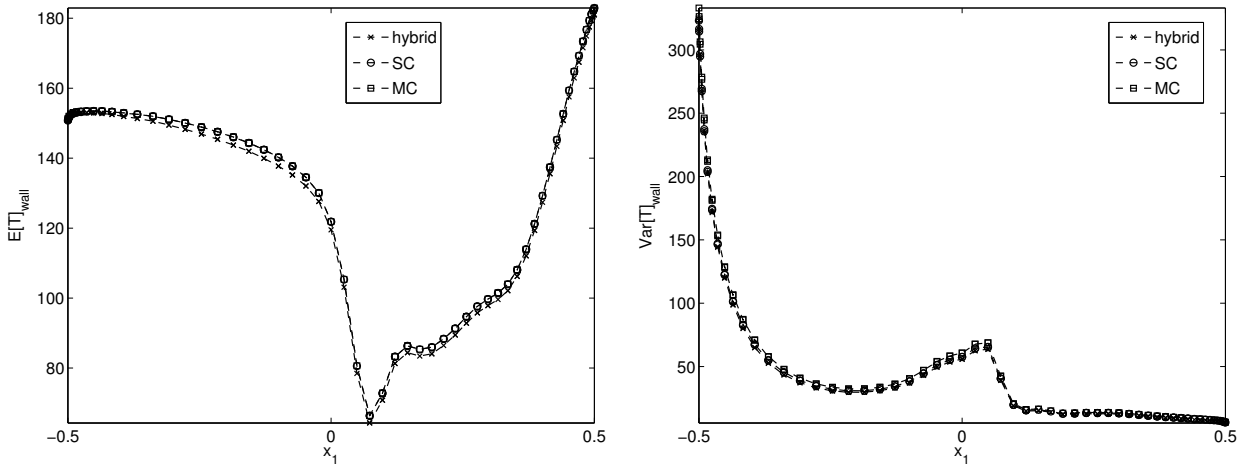

(a) Expectation

(b) Variance

Figure 4. Statistics of temperature along the wall of the cylinder.

and the number of points in the quadrature rules.

References

[1]R. Cameron,W. Martin, The orthogonal development of nonlinear functionals in series of Fourier-Hermite functionals, Ann. of Math. (2), 48 (1947) 385-392.

[2]P. Constantine, A. Doostan, G. Iaccarino, Assessing stochastic collocation methods for analysis of turbulent flow around cylinders, submitted, 2008.

[3]Fluent Inc., FLUENT 6.1 Users Guide, Lebanon, New Hampshire, 2003.

[4]F. R. Menter, Zonal two equation k-w turbulence model predictions, AIAA 93-2906, 1993.

[5]B. Ganapathysubramanian, N. Zabaras, Sparse grid collocation schemes for stochastic natural convection problems, J. Comput. Phys. (2007), doi:10.1017/j.jcp.2006.12.014

[6]F. Nobile, R. Tempone and C.G. Webster. A sparse grid stochastic collocation method for partial differential equations with random input data. Report number: TRITA-NA 2007:07. To appear SINUM.

[7]R. Ghanem,P. Spanos, Stochastic Finite Elements: A Spectral Approach, Springer-Verlag, New York, 1991.

[8]D. Xiu, J.S. Hesthaven, High order collocation methods for the differential equations with random inputs, SIAM J. Sci. Comput. 27 (2005) 1118-1139.

[9]D. Xiu, G. Karniadakis, The Wiener-Askey polynomial chaos for stochastic differential equations, SIAM J. on Sci. Comput., 24 (2002) 619-644.

[10]N. Wiener, The homogeneous chaos, Amer. J. Math., 60 (1938) 897-936.